

## RADIOCARBON LEVELS IN THE ICELAND SEA FROM 25–53 KYR AND THEIR LINK TO THE EARTH'S MAGNETIC FIELD INTENSITY

Antje H L Voelker<sup>1,2</sup> • Pieter M Grootes<sup>1</sup> • Marie-Josée Nadeau<sup>1</sup> • Michael Sarnthein<sup>3</sup>

**ABSTRACT.** By correlating the climate records and radiocarbon ages of the planktonic foraminifera *N. pachyderma*(s) of deep-sea core PS2644 from the Iceland Sea with the annual-layer chronology of the GISP2 ice core, we obtained 80 marine <sup>14</sup>C calibration points for the interval 11.4–53.3 ka cal BP. Between 27 and 54 ka cal BP the continuous record of <sup>14</sup>C/cal age differences reveals three intervals of highly increased <sup>14</sup>C concentrations coincident with low values of paleomagnetic field intensity, two of which are attributed to the geomagnetic Mono Lake and Laschamp excursions (33.5–34.5 ka cal BP with maximum 550‰ marine  $\Delta^{14}\text{C}$ , and 40.3–41.7 ka cal BP with maximum 1215‰ marine  $\Delta^{14}\text{C}$ , respectively). A third maximum (marine  $\Delta^{14}\text{C}$ : 755‰) is observed around 38 ka cal BP and attributed to the geomagnetic intensity minimum following the Laschamp excursion. During all three events the  $\Delta^{14}\text{C}$  values increase rapidly with maximum values occurring at the end of the respective geomagnetic intensity minimum. During the Mono Lake Event, however, our  $\Delta^{14}\text{C}$  values seem to underestimate the atmospheric level, if compared to the <sup>36</sup>Cl flux measured in the GRIP ice core (Wagner et al. 2000) and other records. As this excursion coincides with a meltwater event in core PS2644, the underestimation is probably caused by an increased planktonic reservoir age. The same effect also occurs from 38.5 to 40 ka cal BP when the meltwater lid of Heinrich Event 4 affected the planktonic record.

### INTRODUCTION

Radiocarbon ages have been calibrated in great detail up to 13.3 ka BP by dendro- and varve chronology with an extension based on single calibration points on corals and less precise varves up to 20 ka BP (Stuiver et al. 1998; Bard et al. 1998; Hughen et al. 1998). Beyond 20 ka BP, calibration is still problematic because dendrochronological calibration points are so far not available and single calibration points (Vogel 1983; Bischoff et al. 1994; Vogel and Kronfeld 1997; Bard et al. 1998; Geyh and Schlüchter 1998; Schramm et al. 2000) often lack the needed temporal resolution. A time scale for <sup>14</sup>C ages older than 14 ka BP can be provided by marine or lacustrine varves (e.g. Kitagawa and van der Plicht 1998a, 1998b) or indirectly by the annual-layer chronology of the GISP2 ice core (e.g. Voelker et al. 1998). Calibration data from marine sediment core PS2644 from the western Iceland Sea (67°52.02'N, 21°45.92'W, 777 m water depth; Figure 1) for the interval 20–55 ka cal BP reveal periods with significantly increased atmospheric <sup>14</sup>C concentrations, expressed as  $\Delta^{14}\text{C}$ , the relative deviation from the modern standard <sup>14</sup>C concentration in per mil, during minima in the earth's geomagnetic field intensity (Voelker et al. 1998; Voelker 1999). Increased <sup>14</sup>C production is corroborated by coinciding peaks in <sup>10</sup>Be and <sup>36</sup>Cl in the Greenland ice cores (Yiou et al. 1997; Baumgartner et al. 1997, 1998). We report here further data increasing the temporal resolution of the changes in marine <sup>14</sup>C ages during the Laschamp and Mono Lake excursions and a refinement of the correlation with the GISP2 time scale. A stacked record of the geomagnetic field intensity (NAPIS-75; Laj et al. 2000), including the magnetic data of core PS2644, permits us a direct comparison of our  $\Delta^{14}\text{C}$  fluctuations with changes in the geomagnetic field intensity.

Marine sediment core PS2644 yielded a high resolution climate record showing millennial-scale oscillations (Voelker et al. 1998; Voelker 1999). By correlating the marine climate signals, especially the planktonic  $\delta^{18}\text{O}$  and  $\delta^{13}\text{C}$  records, with the Dansgaard-Oeschger cycles in the GISP2  $\delta^{18}\text{O}$  record we are able to calibrate the marine <sup>14</sup>C ages with the annual-layer GISP2 chronology (Meese et al. 1994, 1997; Bender et al. 1994). Here we assume fluctuations in the temperature on Greenland

<sup>1</sup>Leibniz-Labor für Altersbestimmung und Isotopenforschung, Universität Kiel, Max-Eyth Strasse 11-13, D-24118 Kiel, Germany

<sup>2</sup>Email: antje@sfb313.uni-kiel.de

<sup>3</sup>Institut für Geowissenschaften, Universität Kiel, Olshausenstrasse 40, D-24118 Kiel, Germany

are linked to changes in the hydrography at site PS2644 via the thermohaline circulation (THC) of the North Atlantic. As moisture for the precipitation on Greenland mainly originates from the North Atlantic (Johnsen et al. 1989; Charles et al. 1994; Jouzel et al. 1997), the snow's oxygen isotope ratio should monitor changes in the Sea Surface Temperature (SST) of the major North Atlantic warm water current, the Gulfstream/North Atlantic drift and its branches (e.g. Schmitz and McCartney 1993). One of these branches, the Irminger current, flows partly across the Denmark Strait into the Iceland Sea, and influences site PS2644 (Figure 1). The hydrography at this site is furthermore affected by the polar East Greenland current and its branches (Voelker et al. 1998), which also is part of the North Atlantic THC.

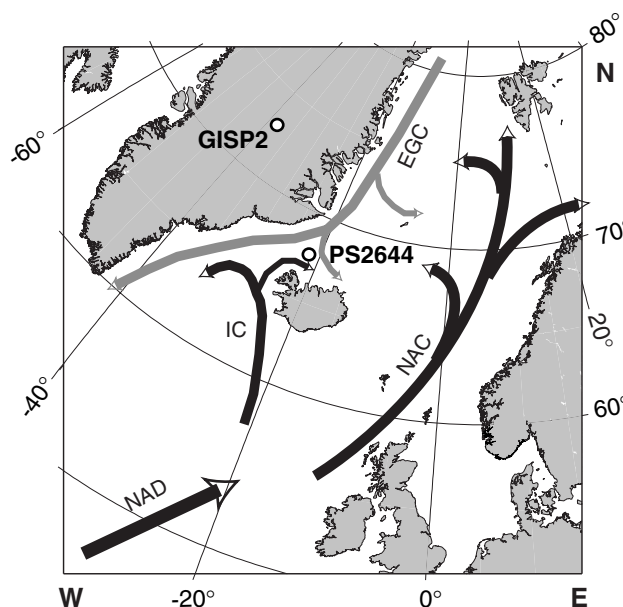


Figure 1 Map of the North Atlantic with the position of sediment core PS2644 in the western Iceland Sea and of ice core GISP2 on Greenland. Arrows mark present axis of the major surface water currents with black ones transporting warm and saline Atlantic water and gray ones fresh and cold polar water (EGC: East Greenland Current; IC: Irminger Current; NAC: Norwegian Atlantic Current; NAD: North Atlantic Drift).

## METHODS

The sediment record of core PS2644 was sampled with a resolution of 1 cm, equal to a mean time resolution of 50 yr during marine isotope stage 3 (29–58 ka cal BP) (Voelker et al. 1998). The stable isotope ratios  $^{18}\text{O}/^{16}\text{O}$  and  $^{13}\text{C}/^{12}\text{C}$  were measured on the planktonic foraminifera *N. pachyderma*(s) in the Leibniz Labor at Kiel University, Germany, using an automated MAT-251 mass spectrometer with carbonate system (analytical reproducibility:  $\pm 0.07\text{‰}$  for  $\delta^{18}\text{O}$ ,  $\pm 0.04\text{‰}$  for  $\delta^{13}\text{C}$ , Samthein et al. 1995; Voelker et al. 1998). Paleoceanographic conditions and climate were reconstructed from a suite of sediment properties including faunal assemblages, stable isotopes, lithology and the abundance of ice rafted detritus (IRD) indicated by lithic grains  $>150\text{ }\mu\text{m}$  which includes the volcanic ash grains, although some were probably wind transported (Voelker 1999; data at <http://www.pan-gaea.de>). The AMS  $^{14}\text{C}$  ages were measured on 10-mg samples of either the planktonic foraminifera

*N. pachyderma*(s) or the epibenthic foraminifera *Cibicides* sp. (for details see Voelker et al. 1998) at the Leibniz Labor at Kiel University. Careful cleaning and sample preparation (Schleicher et al. 1998; Nadeau et al. forthcoming) and the use of *N. pachyderma*(s) samples from marine isotope stage 5.1 of core PS2644 for background correction (Voelker et al. 1998; Voelker 1999) allowed dating of the record up to 55 ka BP. Age differences are calculated by subtracting the  $^{14}\text{C}$  age not corrected for a reservoir effect from the corresponding GISP2 calendar age, alternatively, the relative deviation of the original  $^{14}\text{C}$  concentration.  $\Delta^{14}\text{C}$  in per mil, also based on the uncorrected  $^{14}\text{C}$  ages, is referred to as “marine  $\Delta^{14}\text{C}$ ” to clearly distinguish it from the generally used atmospheric  $\Delta^{14}\text{C}$ .

The  $\delta^{18}\text{O}_{\text{ice}}$  of the GISP2 ice core, calibrated to VSMOW, was measured in the Quaternary Isotope Laboratory in Seattle (USA) (Grootes et al. 1993; Grootes and Stuiver 1997; Stuiver and Grootes 2000). Here we use the bidecadal data set which is based on the 20-cm resolution record (equal to an average time resolution of 12 yr during interstadials and 30 yr during stadials; Stuiver and Grootes [2000]; data available from [http://depts.washington.edu/qil/datasets/gisp2\\_main.html](http://depts.washington.edu/qil/datasets/gisp2_main.html)).

### Correlation with the GISP2 Isotope Record

Since cores PS2644 and GISP2 both monitor changes in the thermohaline circulation of the North Atlantic, the best way to correlate them would be via a sea surface temperature record (e.g. Sachs and Lehman 1999; van Kreveland et al. 2000). Unfortunately, the diversity in the planktonic foraminifera fauna in core PS2644 in the northern North Atlantic is so small (*N. pachyderma*(s) >95%) that they can only be used as qualitative SST indicator (Voelker et al. 1998) forcing us to use the planktonic isotope record instead. This shows light  $\delta^{18}\text{O}$  and  $\delta^{13}\text{C}$  values together with high IRD contents (Figure 2) during cold SST's in the North Atlantic and cold temperatures above Greenland contemporary with meltwater events (Bond et al. 1993; Rasmussen et al. 1996; van Kreveland et al. 2000). The response of precipitation on Greenland to changes in the THC in the northern North Atlantic is immediate as both are connected by the atmospheric circulation. At site PS2644, an “overshooting” SST upon warming is caused by the resumed inflow of warm Atlantic water via the Irminger Current as evidenced by lower percentages of *N. pachyderma*(s) and by high abundances of (Atlantic) radiolaria and diatoms (Voelker et al. 1998; Voelker 1999; Lein 1998). Meltwater lids, on the other hand, hampered the heat transport to the north and induced a sea ice cover during at least part of the year (Sarnthein et al. 1995; Seidov et al. 1996; Cortijo et al. 1997; Voelker 1999).

The detailed tuning of the marine and the ice core followed this hierarchy: Four tephra layers (1) build a stable time frame for the correlation of the Heinrich meltwater events 1–6 (2), other meltwater events contemporary with an increased IRD content (3), and the beginning of the interstadials (4). Further tie points are based on “minor” meltwater events occurring during the interstadials (5), and finally small scale oscillations (6).

1. The tephra layers were identified in the sediment and the GISP2 or GRIP ice core on the base of their chemistry (Voelker 1999; Grönvold et al. 1995; Zielinski et al. 1997). While ash grains of the Saksunarvatn Ash (10,272 GISP2 cal yr) and the North Atlantic Ash Zone 2 (53,260 GISP2 cal yr) were directly detected in the GISP2 core, the ages of the Vedde Ash (12,095 GISP2 cal yr) and a Katla Ash (78,080 GISP2 cal yr), both detected only in GRIP, were obtained by matching the isotope records of both ice cores.
2. Following Bond et al. (1993) and Rasmussen et al. (1996), the Heinrich Events, the most prominent planktonic  $\delta^{18}\text{O}$  minima in core PS2644 (Figure 2; Voelker et al. 1998), were related to the stadial phases preceding Dansgaard-Oeschger Events 1, 2, 4, 8, 12, and 17 in the same way as described in the next paragraph.

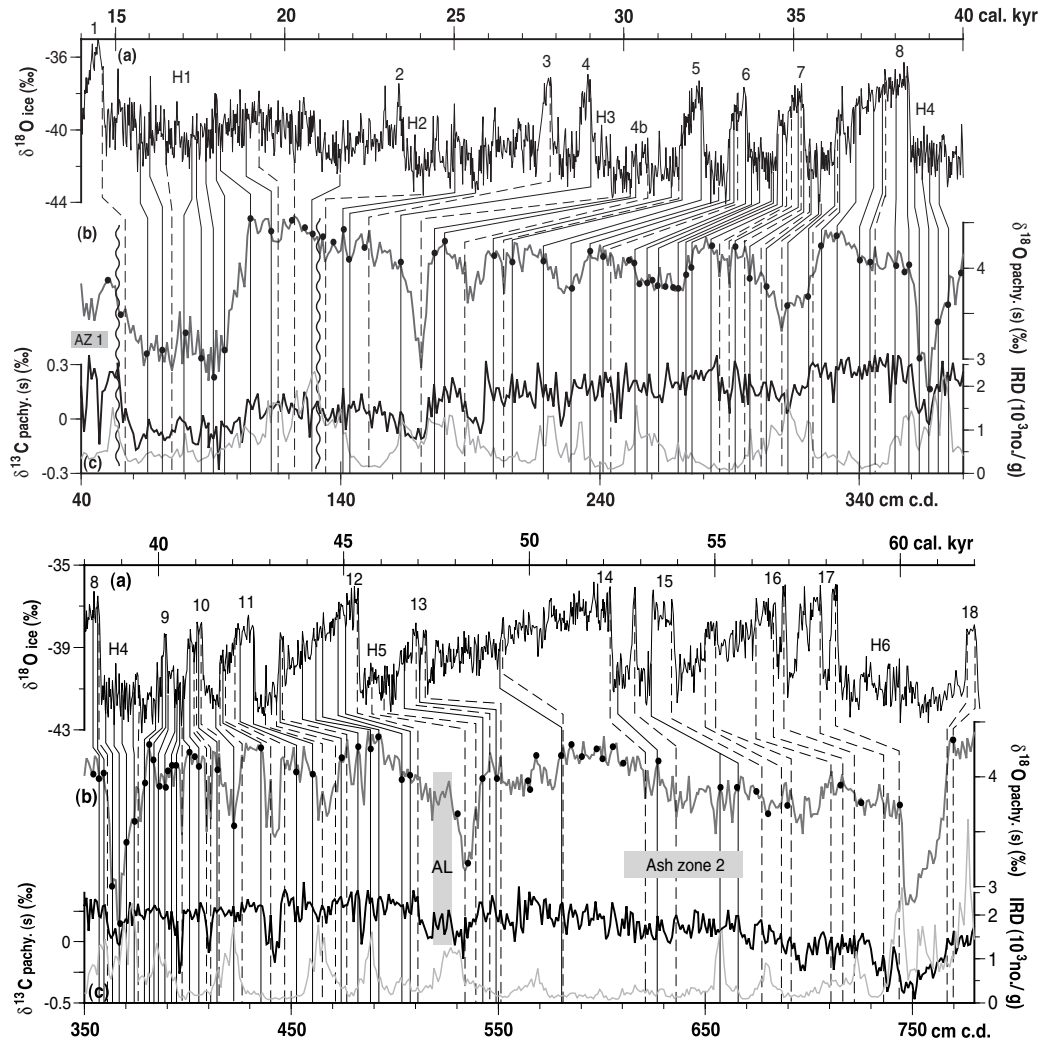


Figure 2 Correlation (vertical lines; dashed, if no calibration point) between planktonic  $\delta^{18}\text{O}$  (b; ‰ vs. VPDB),  $\delta^{13}\text{C}$  (c; black curve; ‰ vs. VPDB), and IRD (c; gray curve; nr. of lithic grains  $>150\mu\text{m/g}$ ) records of sediment core PS2644 vs. composite depth (c.d.) and the bidecadal  $\delta^{18}\text{O}$  record of ice core GISP2 (a; ‰ vs. VSMOW; Stuiver and Grootes 2000). Numbers in (a) refer to Dansgaard-Oeschger Events 1–18 (Johnsen et al. 1992), H1–H6 to Heinrich Events 1–6. Black dots in (b) mark depths of  $^{14}\text{C}$  ages. (A): 14–40 ka BP; wavy line indicates hiatus (Voelker et al. 1998; Voelker 1999); AZ 1: North Atlantic Ash zone 1. (B): 38–62 ka BP; Ash zone 2: North Atlantic Ash zone 2; AL: ash layer.

- Core PS2644 shows several other meltwater events which can be divided into two groups: those contemporary with an increased IRD content, and those without one (Figure 2). Following the feature of the Heinrich Events, we regard the meltwater events with IRD sedimentation north of the Denmark Strait to influence the climate basin-wide and thus tie them to the other stadial phases in the GISP2  $\delta^{18}\text{O}$  record. Since it is difficult to define the first cold point of a stadial in the marine records, the preceding rapid temperature change at the interstadial/stadial transition, is used as anchor point instead. Thereby, we correlate the last heavy planktonic  $\delta^{18}\text{O}/\delta^{13}\text{C}$  value before an IRD-bearing meltwater event with the beginning of the abrupt temperature drop on

- Greenland (Figure 2). Furthermore, the  $\delta^{18}\text{O}$  minimum of a meltwater event is matched with the coldest (i.e. most negative) point prior to the rapid temperature rise in the GISP2  $\delta^{18}\text{O}$  record.
4. The stadial/interstadial transition is marked by a rapid temperature rise on Greenland and a rapid and contemporary increase in the planktonic  $\delta^{18}\text{O}/\delta^{13}\text{C}$  values in core PS2644. The heavy planktonic values indicate a well-ventilated upper ocean layer, ergo the disappearance of the meltwater lid, and are therefore related to the end of the temperature rise (Figure 2). At interstadial 12, this principle of correlation was slightly modified based on the assumption that the pronounced ash layer largely enhanced the sedimentation rate and thus influenced the climate signals (Figure 2B; Voelker 1999).
  5. Like the IRD-bearing meltwater events tied to the stadials, the “no IRD” events, with a presumed lesser climatic impact, are related to temperature drops within an interstadial in the way that the heavy  $\delta^{18}\text{O}/\delta^{13}\text{C}$  values prior to the meltwater event are linked to the last “warm” point preceding the drop, the planktonic  $\delta^{18}\text{O}$  minimum to peak cold, and the heavy values following the meltwater event to the subsequent warming (Figure 2).
  6. Finally, to calibrate almost all  $^{14}\text{C}$  ages with corresponding GISP2 calendar ages we applied the rules of heavy planktonic isotope values indicating warmer, better climate conditions and light values colder temperatures also to small scale oscillations (Figure 2).

Our correlation was recently confirmed by the position of the short Mono Lake excursion in relation to the Dansgaard-Oeschger stadial/interstadial cycles within core PS2644 (stadial prior to Dansgaard-Oeschger Event 6; Figure 3). Wagner et al. (2000) observe an increased  $^{36}\text{Cl}$  flux in the GRIP ice core which is attributed to the Mono Lake intensity minimum exactly at the same position. During the longer lasting Laschamp Event, our correlation also matches the peak fluxes of cosmogenic isotopes in the GRIP ice core (Yiou et al. 1997; Baumgartner et al. 1998) with the inclination swing in core PS2644 (Voelker et al. 1998).

### **Limitations of the Calibration Data**

The calibration data from core PS2644 are affected by three limiting factors (discussed below): uncertainty in the GISP2 calendar ages, smoothing by bioturbation, and changes in the reservoir age.

#### *GISP2 Time Scale*

The calendar ages used to calculate the  $^{14}\text{C}$  deviations are based on the Meese/ Sowers time scale for the GISP2 ice core. Down to 50 ka cal BP, this time scale derives purely from annual-layer counting (Meese et al. 1994, 1997), while, beyond 50 ka cal BP, trace gas concentrations are used to correlate the Vostok chronology of Sowers et al. (1993) into the GISP2 ice core (Bender et al. 1994). The uncertainty on the time scale increases with depth and amounts to an estimated maximum  $\pm 2\%$  up to 39,852 cal BP, maximum  $\pm 5\text{--}10\%$  up to 44,583 cal BP and maximum  $\pm 10\%$  up to 56,931 cal BP (Meese et al. 1997).

For the last 46 ka cal BP, i.e. the main part of our calibration curve, the validity of the GISP2 layer chronology is corroborated by the counted time scale of the nearby GRIP ice core (Hammer et al. 1997) and U/Th dates of coral terraces in Papua New Guinea (Chappell et al. 1996; Grootes and Stuiver 1997). In the older section, the GISP2 chronology might be too young as indicated by the U/Th age of the coral reef associated with Dansgaard-Oeschger interstadial 14, which is 1 ka older, and by other dates of the North Atlantic Ash Zone 2. The ignimbrite attributed to this ash zone was Ar/Ar dated with  $55 \pm 2$  ka (Sigurdsson personal communication 1998), while the tephra is dated even older at 58.38 ka cal BP in the GRIP layer chronology (Hammer et al. 1997). However, since the different age determinations agree within the error bars, the GISP2 chronology is not wrong.

### Bioturbation

As in any oxygenated sediment record, bioturbation works as a low-pass filter and thus hampers a precise reconstruction of the  $^{14}\text{C}$  production over time by dampening the response. In marine cores, the mixed layer depth partly depends on the flux of organic carbon ( $C_{\text{org}}$ ) to the sea floor (Trauth et al. 1997 and references therein). Based on the low  $C_{\text{org}}$ -flux Trauth, Sarnthein and Arnold (1997) postulate bioturbation depths of around 2 cm for sediment cores in the northern Norwegian Sea. Using their approach and the  $C_{\text{org}}$  accumulation rates of core PS2644 (average AR = 0.05 gC/m<sup>2</sup> yr; Stein unpublished data), the average mixed layer depth would be even lower (<1 cm) in the western Iceland Sea. At an average sedimentation rate of 20 cm/ka during isotope stage 3, bioturbation would thus hardly dampen the record of  $^{14}\text{C}$  production. Accordingly, from the view point of bioturbation/mixing alone the response time in the ocean and the atmosphere would nearly be the same (50–100 yr in core PS2644 and 80 yr in the atmosphere). On the other hand, in isotope stage 2 where the sedimentation rates are much lower (Voelker 1999), a delay in the marine response of up to 250 yr might occur.

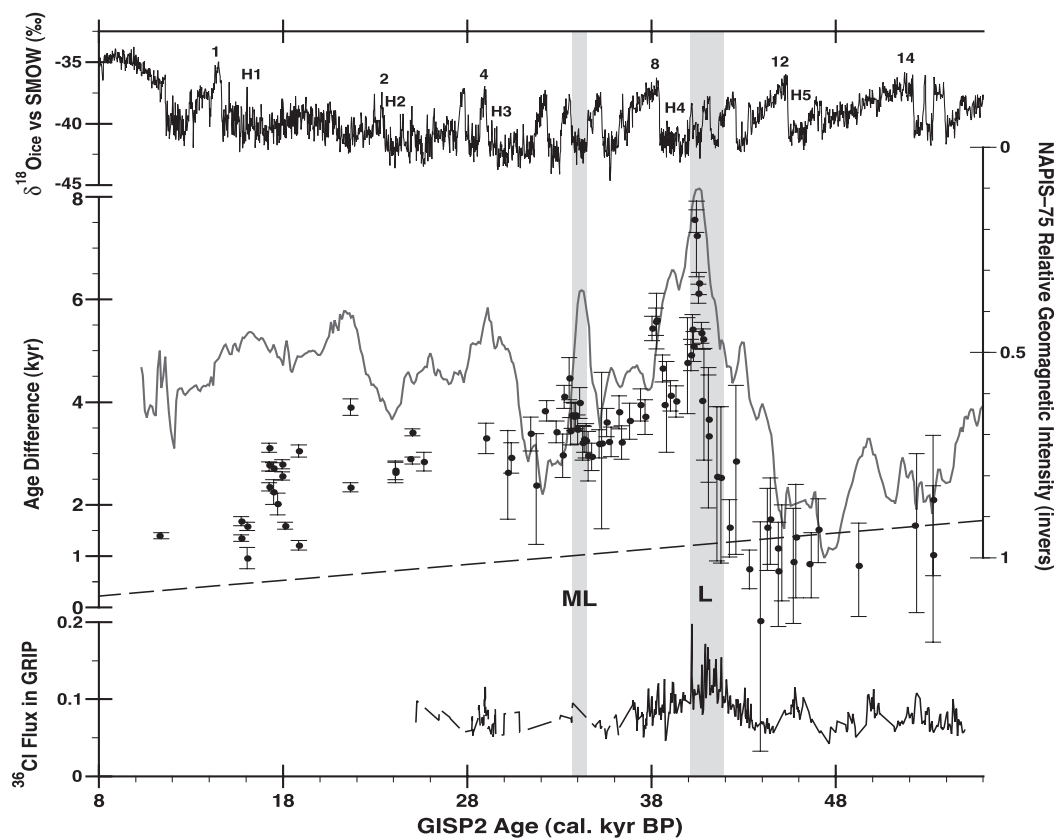


Figure 3 Age differences ( $\pm 1\sigma$ ) between uncorrected  $^{14}\text{C}$  (in Libby yr) and calendar ages on the GISP2 calendar age scale in comparison to the GISP2  $\delta^{18}\text{O}$  record (upper panel: major Dansgaard-Oeschger and Heinrich (H) events 1–6), the (inversed) NAPIS-75 stack of Laj et al. (2000; normalized to 1; gray), and the  $^{36}\text{Cl}$  flux in GRIP (lower panel: Baumgartner et al. 1998; dashed line indicates lower resolution). The  $^{36}\text{Cl}$  record, originally based on the Johnson time scale, was adjusted to the GISP2 time scale by adding 2580 years (fit of maximum flux to peak of Dansgaard-Oeschger Event 9). Dashed ascending line shows difference between conventional and physical  $^{14}\text{C}$  ages. Gray bars indicate Mono Lake (ML) and Laschamp (L) excursions.

### Variation of the Reservoir Effect

The temporal variation of the reservoir effect is hardly known for the northern North Atlantic—except for the Younger Dryas when it increased from 400 to 800–1100 yr (Bard et al. 1994; Hafliðason et al. 1995). Based on atypical negative differences between benthic and planktonic  $^{14}\text{C}$  ages from the same depth in core PS2644, Voelker et al. (1998) postulated fluctuating and increased reservoir ages for planktonic foraminifera in the western Iceland Sea during marine isotope stage 2. According to them, values for the planktonic reservoir age ranged between 630 and 1160 yr during Heinrich Event 1 (14.6–18.1 ka cal BP), rose up to 2240 yr during the last glacial maximum (LGM) and amounted to 950 yr around 25 ka cal BP. The large discrepancy between the benthic and planktonic reservoir age can be explained by the hydrographic conditions in the glacial Nordic Seas and the preferred living conditions of *N. pachyderma*(s). *N. pachyderma*(s) builds a second calcite crust, which contributes about 50% to the shell weight (Arikawa 1983), within or underneath the thermocline (Kohfeld et al. 1996; Simstich 1999). Therefore, its reservoir age highly depends on the ventilation of the thermocline and upper intermediate water. As indicated by the relatively low planktonic  $\delta^{13}\text{C}_{\text{DIC}}$  values (0.7–1.0‰), this water was poorly ventilated during glacial times when a meltwater lid and/or sea ice covering the western Iceland and Greenland Seas hindered the exchange with the atmosphere (Sarnthein et al. 1995; Voelker 1999). Furthermore, “fossil”  $\text{CO}_2$  originating either from stranded icebergs melting near site PS2644 or directly from the melting Greenland ice sheet and shelves, might have biased the  $^{14}\text{C}$  concentration in the (sub)surface water, similar to the modern situation underneath the Antarctic ice shelves (Domack et al. 1989). The deep water, on the other hand, was newly convected in the Norwegian Sea as evidenced by heavy benthic  $\delta^{18}\text{O}$  values (Duplessy et al. 1988; Dokken and Jansen 1999) and flowed—at least partly—across the Iceland Plateau and the Denmark Strait where it was recorded in epibenthic  $\delta^{18}\text{O}$  values of up to 5.55‰, benthic  $\delta^{13}\text{C}_{\text{DIC}}$  values of 1.5–1.7‰ (Voelker 1999) and younger  $^{14}\text{C}$  ages. Since we assume the benthic  $^{14}\text{C}$  ages during marine isotope stage 2 to originate from a young water mass, their  $\Delta^{14}\text{C}$  levels, higher than those of *N. pachyderma*(s) (Table 1), should be closer to the actual atmospheric level.

According to high resolution planktonic and benthic isotope curves (Rasmussen et al. 1996; Dokken and Jansen 1999; Voelker 1999 and unpublished data) hydrographic conditions similar to the LGM also occurred during marine isotope stage 3 in the Nordic Seas and might have led to large fluctuations in the reservoir effect e.g. during Heinrich Event 4 (Sarnthein et al., forthcoming). So, because these variations in the reservoir effect cannot be quantified, our data set cannot be connected to the atmospheric values. Instead, it represents a calibration set for the local upper ocean reflecting the atmospheric changes, but modified by the local oceanography.

### Variation of the Age Differences (Marine $\Delta^{14}\text{C}$ )

The differences between the Libby  $^{14}\text{C}$  ages, not corrected for the reservoir effect, and the GISP2 calendar ages vary between –260 and 7530 years, equal to –170 to +1215‰ marine  $\Delta^{14}\text{C}$  (Figure 3; Table 1). During the interval 43–53.3 ka cal BP most age differences would actually be negative—like the marine  $\Delta^{14}\text{C}$  values—when the 3% offset between Libby- and physical  $^{14}\text{C}$ -years is taken into account (Figure 3). However, starting around 46 ka cal BP ( $\approx 45$  ka BP) the age differences increase steadily until 40.4 ka cal BP ( $\approx 33$  ka BP) whereby the major rise from  $\approx 2500$  to  $>7200$  yr (marine  $\Delta^{14}\text{C}$ : 183–1215‰) is confined to the much shorter period from 41.5 to 40.4 ka cal BP. This rapid increase coincides with the Laschamp inclination swing and drop in geomagnetic intensity in core PS2644 (Figure 4; Voelker et al. 1998; Laj et al. 2000) and with the highest  $^{10}\text{Be}$  (Yiou et al. 1997) and  $^{36}\text{Cl}$  fluxes in the GRIP ice core (Figure 3; Baumgartner et al. 1998). After the  $\Delta^{14}\text{C}$  maximum at the end of the Laschamp excursion the age differences immediately drop to  $\approx 5000$  years

( $\leq 704\text{‰}$ ) during Dansgaard-Oeschger Event 9 and even lower during Heinrich Event 4 (H4; Figures 3, 4). During H4, the marine  $\Delta^{14}\text{C}$  values seem to be dampened by an increased reservoir age. This is inferred because as soon as the meltwater disappeared at the beginning of Dansgaard-Oeschger interstadial 8 (38 ka cal BP/ $\approx 32.6$  ka BP) the age differences reached a second maximum of 5600 yr (755‰). This second peak coincides with the end of the weaker magnetic intensity minimum following the Laschamp Event thereby marking the end of the high  $^{14}\text{C}$  production period between 42 and 38 ka cal BP (Figures 3, 4).

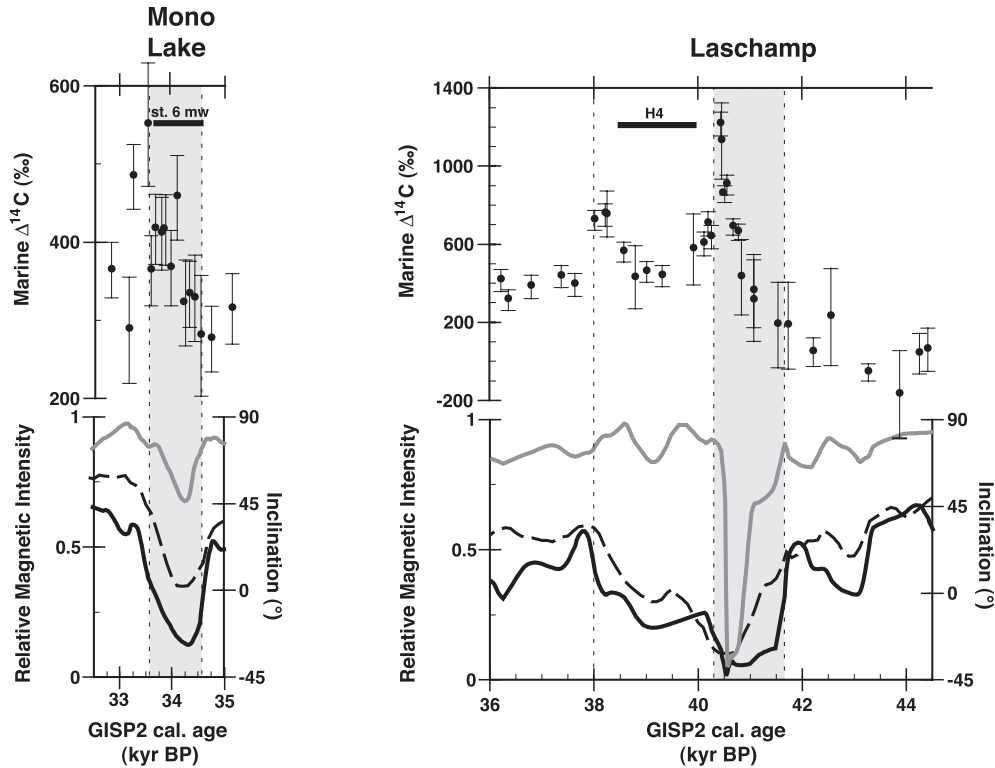


Figure 4 Close-up of marine  $\Delta^{14}\text{C}$  values ( $\pm 1\sigma$ ; upper panel), magnetic records of core PS2644 (lower panel; gray: inclination; black: normalized relative geomagnetic intensity based on  $\text{NRM}/\text{ARM}/10^3$ ; Voelker et al. 1998), and the NAPIS-75 stack (dashed line in lower panel; Laj et al. 2000) vs. GISP2 calendar age (ka BP) for the Mono Lake and Laschamp Event. Horizontal black bar indicates interval of meltwater event during stadial 6 (st.6 mw) or Heinrich Event 4 (H4). Gray bars mark the interval of Mono Lake or Laschamp excursion, thinly dashed lines mark the beginning and end of major geomagnetic intensity minima.

After 38 ka cal BP the age differences decline to values around 3700 years ( $\approx 400\text{‰}$ ) and even further after 35.3 ka cal BP down to around 3000 years ( $\approx 300\text{‰}$ ) (Figure 3; Table 1). The slow but steady  $\Delta^{14}\text{C}$  decrease is interrupted by a third brief maximum between 34.5 and 33.5 ka cal BP ( $\approx 29\text{--}30$  ka BP), which is contemporary with the Mono Lake intensity minimum (Figure 4; Voelker et al. 1998; Laj et al. 2000). During this interval, the age anomalies rose continuously until they reached 4470 years (550‰) at the end of the intensity minimum (Figures 3, 4). As the Mono Lake excursion coincides with a meltwater event and the maximum age difference with the beginning of Dansgaard-Oeschger interstadial 6, it is comparable to the interval from 40 to 38.5 ka cal BP ( $\approx \text{H4}$ ).



Accordingly, most marine  $\Delta^{14}\text{C}$  values should be low due to an increased reservoir effect and thereby make us underestimate the true atmospheric  $\Delta^{14}\text{C}$  levels. This assumption is corroborated by the  $^{36}\text{Cl}$  flux data from the GRIP ice core (Wagner et al. 2000) and by a Bahamian speleothem  $^{14}\text{C}$  record (Richards et al. submitted; Beck et al. submitted), both of which show similar values for the Mono Lake and the Laschamp Event, higher than those obtained from core PS2644.

After the Mono Lake Event, the age differences decrease again to values between 3500 and 2500 yr (until 24 ka cal BP/21 ka BP). In the range between 15.7 and 21.6 ka cal BP ( $\approx$ 14–19 ka BP), where our age control is weaker because of subdued climatic signals in cores PS2644 and GISP2 and where the planktonic reservoir age greatly fluctuated, the data points show a large scatter (Figure 3, Table 1).

### **Comparison with Other Records for Ages >20 ka cal BP**

Our  $\Delta^{14}\text{C}$  record, with two major increases between 30 and 55 ka cal BP, is similar to the high resolution  $^{14}\text{C}$ –U/Th record from Bahamian speleothems (Richards et al. submitted; Beck et al. submitted) and a marine record from the Cariaco basin (Hughen et al. 1997). For the range >20 ka cal BP a perfect match between the Bahamian record and the record from core PS2644 would be obtained by shifting the Iceland Sea data by +2000 yr (W Beck personal communication 2000). Since the U/Th dates (W Beck personal communication 2000; J Chappell personal communication 2000) as well as the GISP2 chronology appear reliable further work on the time scales is needed to resolve this age dispensary. This is especially important because the true calendar age also determines  $\Delta^{14}\text{C}$ . Disparity in  $\Delta^{14}\text{C}$  exists during the Mono Lake Event when the Bahamian record shows  $\Delta^{14}\text{C}$  values as high as during the Laschamp interval, just like the  $^{36}\text{Cl}$  flux in the GRIP ice core (Wagner et al. 2000), which indicates the subdued character of the marine  $\Delta^{14}\text{C}$  record. The comparison with the atmospheric record from Lake Suigetsu (Kitagawa and van der Plicht 1998a, 1998b) reveals major discrepancies with the Lake Suigetsu record often being younger, with consequently smaller  $\Delta^{14}\text{C}$  deviations, and, especially, lacking the rapid increase associated with the Laschamp Event. The inconsistency is probably due to an imprecise varve chronology in Lake Suigetsu for the oldest part of the record, as stated by Kitagawa and van der Plicht (1998a).

The calibration data presented here also generally agree with single calibration points of Bard et al. (1998), Geyh and Schlüchter (1998), Schramm et al. (2000), Vogel (1983) and Vogel and Kronfeld (1997) (compilations in Voelker 1999 and Schramm et al. 2000). For the Laschamp Event, however, four calibration points from Bischoff et al. (1994), Geyh and Schlüchter (1998), and Schramm et al. (2000) place the  $\Delta^{14}\text{C}$  rise up to 2000 years earlier than our data. Thereby the declination change associated with the Laschamp Event in the Lake Lisan record is dated to 42.2 U/Th years (Marco et al. 1998 with revised ages from Schramm et al. 2000). Further discrepancies with single calibration data occur between 34.5–35 ka cal BP where Geyh and Schlüchter (1998) and Vogel (1983) observe higher deviations (more in agreement with the Bahamian record).

### **Geomagnetic Control of the $^{14}\text{C}$ Production 25–50 ka BP**

Since  $\text{pCO}_2$  records from Antarctic ice cores reveal variations of only 10–20 ppmv during isotope stages 2 and 3 (Neftel et al. 1988; Indermühle et al. 2000), changes in the global carbon cycle most likely played only a minor role in modulating the  $\Delta^{14}\text{C}$  record. Major changes in North Atlantic deep water formation and the strength of the THC may have produced transient spikes in  $\Delta^{14}\text{C}$  (Goslar et al. 1995; Stocker and Wright 1996, 1998; Hughen et al. 1998). Also, the offset between conventional and physical  $^{14}\text{C}$  ages diminishes the maximal age differences by only 950–1160 yr (Figures 3, 4) so that the major portion of the age anomalies must be attributed to an enhanced and varying  $^{14}\text{C}$  pro-

duction. Increased production, further corroborated by high fluxes of the cosmogenic isotopes  $^{36}\text{Cl}$  and  $^{10}\text{Be}$  (Voelker et al. 1998), was caused by a low geomagnetic field strength which, based on absolute intensity data, was four to ten times lower during the Laschamp Event (4–14  $\mu\text{T}$ ; Roperch et al. 1988; Chauvin et al. 1989; Levi et al. 1990) than at “present” ( $49.2 \pm 12.7 \mu\text{T}$  for 1943–1952 AD; Gonzalez et al. 1997) and about half as low during the Mono Lake Event (19–24  $\mu\text{T}$ ; Gonzalez et al. 1997; Valet et al. 1998). For the interval 27–54 ka cal BP, the similarity between our  $\Delta^{14}\text{C}$  record and the multi core relative intensity record of NAPIS-75 (Laj et al. 2000; Figure 3), the shape of which is confirmed by other high-resolution geomagnetic records from the North Atlantic (Stoner et al. 1995, Channell et al. 1997; Channell 1999), South Atlantic (Channell et al. 2000), and North Pacific (Roberts et al. 1997), provides strong evidence for the predominant geomagnetic modulation of the  $\Delta^{14}\text{C}$  record. While the  $^{14}\text{C}$  production peaks during the geomagnetic intensity minima resulted in apparently too young  $^{14}\text{C}$  ages, the production during the intensity maximum around 47 ka cal BP was probably the lowest during the last 53 ka cal BP and resulted in apparently too old  $^{14}\text{C}$  ages.

## CONCLUSION

The detailed correlation of sediment core PS2644 with the annual-layer chronology of the GISP2 ice core provides us with 70 marine calibration points for the interval 24 to 53.3 ka cal BP. Because at site PS2644 the reservoir age was unknown and probably varied over time, Libby  $^{14}\text{C}$  ages were used for a local marine calibration. The age anomalies probably represent minimum values for the atmospheric  $\Delta^{14}\text{C}$  changes. This is especially true for the intervals from 33.5 to 34.5 ka cal BP and from 38.5 to 40 ka cal BP when meltwater events caused an increased (planktonic) reservoir age and resulted in smaller age anomalies at site PS2644. When a high resolution atmospheric record becomes available in the future, the changes in the reservoir age of the northern North Atlantic can easily be reconstructed by subtracting the marine from the atmospheric record. The three  $\Delta^{14}\text{C}$  maxima concur with minima in the geomagnetic intensity which indicates the cause of the enhanced  $^{14}\text{C}$  production. This is further corroborated by increased flux rates of cosmogenic isotopes in ice cores from the Arctic and Antarctic (Voelker et al. 1998 and references therein; Wagner et al. 2000).

Though our data represent only marine  $\Delta^{14}\text{C}$  levels, they are in general agreement with most other calibration data, especially the rapid  $\Delta^{14}\text{C}$  increase between 44 and 40 ka cal BP and the second  $\Delta^{14}\text{C}$  maximum around 34 ka cal BP. For ages >32 ka cal BP, however, they highly diverge from the Lake Suigetsu record of Kitagawa and van der Plicht (1998), hinting to possible problems in the varve chronology for this time range. The high  $\Delta^{14}\text{C}$  variability during the interval 24–54 ka cal BP revealed by our and most other data clearly shows that a true calibration of  $^{14}\text{C}$  ages >20 ka BP cannot be done by interpolating between a few coral calibration points (Bard et al. 1998). The combined calibration data, however, provide a better base for calibrating  $^{14}\text{C}$  ages >20 ka BP. A new high resolution record based on terrestrial organic carbon dates and a sound calendar age scale are nevertheless necessary to provide true atmospheric  $\Delta^{14}\text{C}$  levels and to allow estimations of changes in the reservoir age in various parts of the world ocean.

## ACKNOWLEDGMENTS

These many  $^{14}\text{C}$  ages could not have been produced without the help of several students who helped to prepare the sediment samples or picked hundreds of foraminifera shells under the microscope for AMS samples. The technical team of the Leibniz laboratory, especially A Oriwall, is warmly thanked for the efficiency and expertise in preparing and running the AMS samples. Helmut Erlenkeuser and his team are thanked for the stable isotope measurements. AV would also like to thank Carlo Laj and Catherine Kissel from LSCE (CEA–CNRS, Gif-sur-Yvette) and Juerg Beer and Ger-

hard Wagner from EAWAG (Dübendorf) for the stimulating collaboration and sharing their data. This study was generously funded by the Deutsche Forschungsgemeinschaft Bonn through the Sonderforschungsbereich 313 at Kiel University.

## REFERENCES

- Arikawa R. 1983. Distribution and taxonomy of globigerina pachyderma (Ehrenberg) off the Sanriku coast, northeast Honshu, Japan. *Scientific Reports Tohoku University, 2nd series (Geology)* 53(2):103–57.
- Bard E, Arnold M, Mangerud J, Paterne M, Labeyrie L, Duprat J, Melieres M-A, Sonstegaard E, Duplessy J-C. 1994. The North Atlantic atmosphere-sea surface  $^{14}\text{C}$  gradient during the Younger Dryas climatic event. *Earth and Planetary Science Letters* 126:275–87.
- Bard E, Arnold M, Hamelin B, Tisnerat-Laborde N, Caubioch G. 1998. Radiocarbon calibration by means of mass spectrometric  $^{230}\text{Th}/^{234}\text{U}$  and  $^{14}\text{C}$  ages of corals: an updated database including samples from Barbados, Mururoa and Tahiti. *INTCAL98: calibration issue. Radiocarbon* 40(3):1085–92.
- Baumgartner S, Beer J, Suter M, Dittrich-Hannen B, Synal H-A, Kubik PW, Hammer C, Johnsen S. 1997. Chlorine 36 fallout in the Summit Greenland Ice Core Project ice core. *Journal of Geophysical Research* 102(C12):26,659–62.
- Baumgartner S, Beer J, Masarik J, Wagner G, Meynadier L, Synal H-A. 1998. Geomagnetic modulation of the  $^{36}\text{Cl}$  flux in the GRIP ice core, Greenland. *Science* 279:1330–32.
- Beck WJ, Richards DA, Donahue DJ, Smart PL, Edwards RL, Herrera-Osterheld S, Burr GS, Calsoyas L, Jull AJT, Biddulph D. Extremely large variations of atmospheric  $^{14}\text{C}$  concentration during marine isotope stage 3. *Science*. Submitted.
- Bender M, Sowers T, Dickson M-L, Orchard J, Grootes P, Mayewski PA, Meese DA. 1994. Climate correlations between Greenland and Antarctica during the past 100,000 years. *Nature* 372:663–66.
- Bischoff JL, Kenneth L, Garcia JF, Carbonell E, Vaquero M, Stafford TW Jr, Jull AJT. 1994. Dating of the basal Aurignacian sandwich at Abric Romani (Catalunya, Spain) by radiocarbon and Uranium-Series. *Journal of Archaeological Science* 21:541–51.
- Bond G, Broecker WS, Johnsen S, McManus J, Labeyrie L, Jouzel J, Bonani G. 1993. Correlations between climate records from North Atlantic sediments and Greenland ice. *Nature* 365:143–47.
- Channell JET. 1999. Geomagnetic paleointensity and directional secular variation at Ocen Drilling Program (ODP) site 984 (Bjorn Drift) since 500 ka: comparisons with ODP site 983 (Gardar Drift). *Journal of Geophysical Research* 104(B10):22,937–951.
- Channell JET, Hodel DA, Lehman B. 1997. Relative geomagnetic paleointensity and  $\delta^{18}\text{O}$  at ODP Site 983 (Gardar Drift, North Atlantic) since 350 ka. *Earth and Planetary Science Letters* 153:103–18.
- Channell JET, Stoner JS, Hodel DA, Charles CD. 2000. Geomagnetic paleointensity for the last 100 kyr from the sub-antarctic South Atlantic: a tool for inter-hemispheric correlation. *Earth and Planetary Science Letters* 175:145–60.
- Chappell J, Omura A, Esat T, McCulloch M, Pandolfi J, Ota Y, Pillans B. 1996. Reconciliation of late Quaternary sea levels derived from coral terraces at Huon Peninsula with deep sea oxygen isotope records. *Earth and Planetary Science Letters* 141:227–36.
- Charles CD, Rind D, Jouzel J, Koster RD, Fairbanks RG. 1994. Glacial-interglacial changes in moisture sources for Greenland: influences on the ice core record of climate. *Science* 263:508–11.
- Chauvin A, Duncan RA, Bonhommet N, Levi S. 1989. Paleointensity of the earth's magnetic field and K-Ar dating of the Louchadiere volcanic flow (central France): new evidence for the Laschamp excursion. *Geophysical Research Letters* 16(10):1189–92.
- Cortijo E, Labeyrie L, Vidal L, Vautravers M, Chapman M, Duplessy J-C, Elliot M, Arnold M, Turon J-L, Auffret G. 1997. Changes in sea surface hydrology associated with Heinrich Event 4 in the North Atlantic-Ocean between  $40^\circ\text{N}$  and  $60^\circ\text{N}$ . *Earth and Planetary Science Letters* 146:29–45.
- Domack EW, Jull AJT, Anderson JB, Linick TW, Williams CR. 1989. Application of tandem accelerator mass-spectrometer dating to late Pleistocene-Holocene sediments of the East Antarctic continental shelf. *Quaternary Research* 31:277–87.
- Dokken TM, Jansen E. 1999. Rapid changes in the mechanism of ocean convection during the last glacial cycle. *Nature* 401:458–61.
- Duplessy JC, Labeyrie L, Blanc PL. 1988. Norwegian Sea deepwater variations over the last climatic cycle: paleo-oceanographical implications. In: Wanner H, Siegenthaler X, editors. *Long and short term variability of climate*. Heidelberg: Springer Verlag. p 83–116.
- Geyh MA, Schlüchter C. 1998. Calibration of the  $^{14}\text{C}$  time scale beyond 22,000 BP. *Radiocarbon* 40(1):475–82.
- Gonzalez S, Sherwood G, Böhm H, Schnepf E. 1997. Palaeosecular variation in Central Mexico over the last 30,000 years: the record from lavas. *Geophysical Journal International* 130:201–19.
- Goslar T, Arnold M, Bard E, Kuc T, Pazdur MF, Ralska-Jasiewiczowa M, Rozanski K, Tisnerat N, Walanus A, Wicik B, Wieckowski K. 1995. High concentration of atmospheric  $^{14}\text{C}$  during the Younger Dryas cold episode. *Nature* 377:414–17.
- Grönvold K, Oskarsson N, Johnsen S, Clausen HB, Hammer CU, Bond G, Bard E. 1995. Ash layers from Ice-

- land in the Greenland GRIP ice core correlated with oceanic and land sediments. *Earth and Planetary Science Letters* 135:149–55.
- Grootes PM, Stuiver M, White JWC, Johnsen S, Jouzel J. 1993. Comparison of oxygen isotope records from the GISP2 and GRIP Greenland ice cores. *Nature* 366: 552–4.
- Grootes PM, Stuiver M. 1997.  $^{18}\text{O}/^{16}\text{O}$  variability in Greenland snow and ice with  $10^{-3}$  to  $10^5$  year time resolution. *Journal of Geophysical Research* 102(C12): 26,455–70.
- Haflidason H, Sejrup HP, Klitgaard-Kristensen D, Johnsen S. 1995. Coupled response of the Late Glacial climatic shifts of northwest Europe reflected in Greenland ice cores: evidence from the northern North Sea. *Geology* 23(12):1059–62.
- Hammer CU, Andersen KK, Clausen HB, Dahl-Jensen D, Schøtt Hvidberg C, Iversen P. 1997. *The stratigraphic dating of the GRIP Ice Core*. Special report. University of Copenhagen, Denmark: Geophysical Department, Niels Bohr Institute for Astronomic Physics and Geophysics. 14 p.
- Hughen KA, Overpeck JT, Lehman SJ, Southon J, Kashgarian M, Peterson LC. 1997. Radiocarbon change in the Cariaco Basin. Presented. AGU 1997 Fall Meeting, San Francisco, California, 8–12 December. EOS Transactions. Fall Meeting Supplement, F338. *AGU* 78(46).
- Hughen KA, Overpeck JT, Lehman SJ, Kashgarian M, Southon J, Peterson L, Alley R, Sigman DM. 1998. Deglacial changes in ocean circulation from an extended radiocarbon calibration. *Nature* 391:65–8.
- Indermühle A, Monnin E, Stauffer B, Stocker TF, Wahlen M. 2000. Atmospheric  $\text{CO}_2$  concentration from 60 to 20 kyr BP from the Taylor Dome ice core, Antarctica. *Geophysical Research Letters* 27(5):735–8.
- Johnsen SJ, Dansgaard W, White JWC. 1989. The origin of Arctic precipitation under present and glacial conditions. *Tellus* 41B:452–68.
- Johnsen SJ, Clausen HB, Dansgaard W, Fuhrer K, Gundestrup N, Hammer CU, Iversen P, Jouzel J, Stauffer B, Steffensen JP. 1992. Irregular glacial interstadials recorded in a new Greenland ice core. *Nature* 359: 311–3.
- Jouzel J, Alley RB, Cuffey KM, Dansgaard W, Grootes P, Hoffmann G, Johnsen SJ, Koster RD, Peel D, Shuman CA, Stievenar, M, Stuiver M, White J. 1997. Validity of the temperature reconstruction from water isotopes in ice cores. *Journal of Geophysical Research* 102(C12):26,471–88.
- Kitagawa H, van der Plicht J. 1998a. Atmospheric radiocarbon calibration to 45,000 yr BP: Late Glacial fluctuations and cosmogenic isotope production. *Science* 279:1187–90.
- Kitagawa H, van der Plicht J. 1998b. A 40,000-yr varved chronology from Lake Suigetsu, Japan: extension of the radiocarbon calibration curve. *Radiocarbon* 40(1): 505–16.
- Kohfeld KE, Fairbanks RG, Smith SL, Walsh ID. 1996. *Neoglobobadrina pachyderma* (sinistral coiling) as paleoceanographic tracer in polar oceans: evidence from Northeast Water Polynya plankton twos, sediment traps, and surface sediments. *Paleoceanography* 11(6):679–99.
- Laj C, Kissel C, Mazaud A, Channell JET, Beer J. 2000. North Atlantic palaeointensity stack since 75 ka (NAPIS-75) and the duration of the Laschamp Event. *Philosophical Transactions of the Royal Society London* A358:1009–25.
- Lein D. 1998. Die Radiolarien-Gemeinschaften von 52 ka bis 12 ka vor heute im Sedimentkern PS2644 aus dem nördlichen Dänemarkstraße. Diploma thesis. Kiel: 51 p.
- Levi S, Audunsson H, Duncan RA, Kristjansson L, Gillot P-Y, Jakobsson SP. 1990. Late Pleistocene geomagnetic excursion in Icelandic lavas: confirmation of the Laschamp excursion. *Earth and Planetary Science Letters* 96:443–57.
- Marco S, Ron H, McWilliam, MO, Stein M. 1998. High-resolution record of geomagnetic secular variation from Late Pleistocene Lake Lisan sediments (paleo Dead Sea). *Earth and Planetary Science Letters* 161: 145–60.
- Meese DA, Alley RB, Gow AJ, Grootes PM, Mayewski PA, Ram M, Taylor KC, Waddington ED, Zielinski GA. 1994. Preliminary depth-age scale of the GISP2 ice core. *CRREL Special Report 94-1*. Hanover, New Hampshire: Cold Regions Research and Engineering Laboratory. 66 p.
- Meese DA, Gow AJ, Alley RB, Zielinski GA, Grootes PM, Ram M, Taylor KC, Mayewski PA, Bolzan JF. 1997. The GISP2 depth-age scale: methods and results. *Journal of Geophysical Research* 102(C12): 26,411–24.
- Nadeau M-J, Grootes PM, Voelker A, Bruhn F, Duhr A, Oriwall A. Carbonate  $^{14}\text{C}$  background: does it have multiple personalities? *Radiocarbon*. Submitted.
- Neftel A, Oeschger H, Staffelbach T, Stauffer B. 1988.  $\text{CO}_2$  record in the Byrd ice core 50,000–5,000 years BP. *Nature* 331:609–11.
- Rasmussen TL, Thomsen E, Labeyrie L, van Weering TCE. 1996. Circulation changes in the Faeroe-Shetland Channel correlating with cold events during the last glacial period (58–10 ka). *Geology* 24(10):937–40.
- Richards DA, Beck WJ, Donahue DJ, Edwards RL, Silverman BW, Smart PL. Atmospheric radiocarbon before 11 ka using submerged speleothems from the Bahamas. *Science*. Submitted.
- Roberts AP, Lehman B, Weeks RJ, Verosub KL, Laj C. 1997. Relative paleointensity of the geomagnetic field over the last 200,000 years from ODP sites 883 and 884, North Pacific Ocean. *Earth and Planetary Science Letters* 152:11–23.

- Roperch P, Bonhommet N, Levi S. 1988. Paleointensity of the earth's magnetic field during the Laschamp excursion and its geomagnetic implications. *Earth and Planetary Science Letters* 88:209–19.
- Sachs JP, Lehman SJ. 1999. Subtropical North Atlantic temperatures 60,000 to 30,000 years ago. *Science* 286: 756–759.
- Sarnthein M, Jansen E, Weinelt M, Arnold M, Duplessy J-C, Erlenkeuser H, Flatoy A, Johannessen G, Johannessen T, Jung S, Koc N, Labeyrie L, Maslin M, Pflaumann U, Schulz H. 1995. Variations in Atlantic surface ocean paleoceanography, 50–80°N: a time-slice record of the last 30,000 years. *Paleoceanography* 10(6):1063–94.
- Sarnthein M, Statterger K, Dreger D, Erlenkeuser H, Grootsep, Haupt B, Jung S, Kieter T, Kuhn W, Pflaumann U, Schäfer-Neth C, Schulz M, Seidor D, Simstich J, van Kreveld-Alfane S, Vogelsang E, Voelker A, Wenelt M. Fundamental modes and abrupt changes in North Atlantic circulation and climate over the last 60 ky—numerical modelling and reconstruction. Forthcoming. In: Schäfer P, Ritzrau W, Schlüter M, Thiede J, editors. *The Northern North Atlantic: a changing environment*. Springer Verlag, Heidelberg.
- Schleicher M, Grootes PM, Nadeau M-J, Schoon A. 1998. The carbonate  $^{14}\text{C}$  background and its components at the Leibniz AMS facility. *Radiocarbon* 40(1): 85–94.
- Schmitz WJ, McCartney MS. 1993. On the North Atlantic circulation. *Reviews of Geophysics* 31(1):29–49.
- Schramm A, Stein M, Goldstein SL. 2000. Calibration of the  $^{14}\text{C}$  time scale to >40 ka by  $^{234}\text{U}$ – $^{230}\text{Th}$  dating of Lake Lisan sediments (last glacial Dead Sea). *Earth and Planetary Science Letters* 175:27–40.
- Seidov D, Sarnthein M, Statterger K, Prien R, Weinelt M. 1996. North Atlantic ocean circulation during the last glacial maximum and subsequent meltwater event: a numerical model. *Journal of Geophysical Research* 101(C7):16,305–332.
- Simstich J. 1999. Die ozeanische Deckschicht des Europäischen Nordmeeres im Abbild stabiler Isotope unterschiedlicher Planktonforaminiferen. DSc dissertation, University of Kiel, Germany: *Berichte-Reports Institut für Geowissenschaften, Universität Kiel*. Nr 2. 96 p.
- Sowers T, Bender M, Labeyrie L, Martinson D, Jouzel J, Raynaud D, Pichon JJ, Korotkevich A. 1993. A 135,000-year Vostock-Specmap common temporal framework. *Paleoceanography* 8:737–66.
- Stocker TF, Wright DG. 1996. Rapid changes in ocean circulation and atmospheric radiocarbon. *Paleoceanography* 11(6):773–95.
- Stocker TF, Wright DG. 1998. Rapid changes in ocean circulation and atmospheric radiocarbon. *Radiocarbon* 40(1):359–66.
- Stoner JS, Channell JET, Hillaire-Marcel C. 1995. Late Pleistocene relative geomagnetic paleo-intensity from the deep Labrador Sea: regional and global correlations. *Earth and Planetary Science Letters* 134:237–52.
- Stuiver M, Reimer PJ, Bard E, Beck JW, Burr GS, Hughen KA, Kromer B, McCormac G, van der Plicht J, Spurk M. 1998. INTCAL98 Radiocarbon age calibration, 24,000–0 cal BP. *INTCAL98: calibration issue. Radiocarbon* 40(3):1041–83.
- Stuiver M, Grootes PM. 2000. GISP2 oxygen isotope ratios. *Quaternary Research* 53(3):277–84.
- Trauth MH, Sarnthein M, Arnold M. 1997. Bioturbational mixing depth and carbon flux at the seafloor. *Paleoceanography* 12:517–26.
- Valet J-P, Tric E, Herrero-Bervera E, Meynadier L, Lockwood JP. 1998. Absolute paleointensity from Hawaiian lavas younger than 35 ka. *Earth and Planetary Science Letters* 161:19–32.
- van Kreveld S, Sarnthein M, Erlenkeuser H, Grootes PM, Jung S, Nadeau M-J, Pflaumann U, Voelker A. 2000. Potential links between surging ice sheets, circulation changes, and the Dansgaard-Oeschger cycles in the Irminger Sea, 60–18 kyr. *Paleoceanography* 15(4): 425–42.
- Voelker AHL, Sarnthein M, Grootes PM, Erlenkeuser H, Laj C, Mazaud C, Nadeau M-J, Schleicher M. 1998. Correlation of marine  $^{14}\text{C}$  ages from the Nordic Seas with the GISP2 isotope record: implications for  $^{14}\text{C}$  calibration beyond 25 ka BP. *Radiocarbon* 40(1):517–34.
- Voelker AHL. 1999. Zur Deutung der Dansgaard-Oeschger Ereignisse in ultra-hochauflösenden Sedimentprofilen aus dem Europäischen Nordmeer. DSc dissertation, University of Kiel, Germany: *Berichte-Reports, Institut für Geowissenschaften, Universität Kiel*, nr. 9:278p.
- Vogel JC. 1983.  $^{14}\text{C}$  variations during the Upper Pleistocene. *Radiocarbon* 25(2):213–18.
- Vogel JC, Kronfeld J. 1997. Calibration of radiocarbon dates for the late Pleistocene using UTh dates on stalagmites. *Radiocarbon* 39(1):27–32.
- Wagner G, Beer J, Laj C, Kissel C, Masarik J, Muscheler R, Synal H-A. 2000. Chlorine-36 evidence for the Mono Lake Event in the Summit GRIP ice core. *Earth and Planetary Science Letters* 181:1–6.
- Yiou F, Raisbeck GM, Baumgartner S, Beer J, Hammer C, Johnsen S, Jouzel J, Kubik PW, Lestringuez J, Stievenard M, Suter M, Yiou P. 1997. Beryllium 10 in the Greenland Ice Core Project ice core at Summit, Greenland. *Journal of Geophysical Research* 102(C12):26,783–94.
- Zielinski GA, Mayewski PA, Meeker LD, Grönvold K, Germani MS, Whitlow S, Twickler MS, Taylor K. 1997. Volcanic aerosol records and tephrochronology of the Summit, Greenland, ice cores. *Journal of Geophysical Research (Oceans)* 102(C12):26,625–40.

**APPENDIX**Table 1 Marine calibration points derived from core PS2644<sup>a</sup>

Composite depth <sup>b</sup> (cm)	Lab code (KIA-)	<sup>14</sup> C age $\pm 1 \sigma$ (yr BP)	GISP2 calendar age (yr BP)	Age difference (yr)	Marine $\Delta^{14}\text{C}^c$ (‰)
22	74	9980 $\pm$ 60	11,390	1410	145.0
65	802	14,370 $\pm$ 60	15,720	1350	119.3
65 (b)	741	14,050 $\pm$ 90	15,720	1670	164.8
71	77	15,080 $\pm$ 210	16,040	960	65.1
71 (b)	1649	14,450 $\pm$ 80	16,040	1590	152.0
80	736	14,890 $\pm$ 80	17,240	2350	261.0
80 (b)	742	14,130 $\pm$ 90	17,240	3110	386.1
80 (b)	743	14,490 $\pm$ 90	17,240	2750	325.3
86	78	15,210 $\pm$ 240	17,460	2250	244.4
86 (b)	1650	14,720 + 90/-80	17,460	2740	322.7
91	79	15,660 + 220/-210	17,680	2020	208.3
95	737	15,380 $\pm$ 80	17,940	2560	291.2
95 (b)	744	15,150 $\pm$ 90	17,940	2790	328.7
105	803	16,510 $\pm$ 70	18,100	1590	143.7
113	804	17,630 $\pm$ 90	18,840	1210	88.0
113 (b)	1641	15,790 $\pm$ 120	18,840	3050	368.0
129	806	19,300 $\pm$ 90	21,640	2340	240.0
129 (b)	745	17,740 $\pm$ 160	21,640	3900	505.8
134 <sup>d</sup>	[1647/710]	21,410 $\pm$ 180	24,080	2670	281.0
134 (b) <sup>d</sup>	[746/747]	21,450 $\pm$ 200	24,080	2630	274.6
141	5373	22,140 $\pm$ 70	25,000	2860	307.4
141 (b)	5374	21,590 $\pm$ 70	25,000	3410	400.1
143	738	22,780 $\pm$ 180	25,620	2840	301.3
163	739	25,700 + 300/-290	29,000	3300	361.7
176	81	27,550 + 910/-820	30,180	2630	247.6
180	740	27,440 + 300/-290	30,360	2920	292.6
199	758	28,030 + 340/-320	31,420	3390	365.4
206	82	29,340 + 1150/-1010	31,720	2380	202.8
218	808	28,470 $\pm$ 200	32,300	3830	437.8
229	809	29,400 $\pm$ 210	32,820	3420	363.7
236	759	30,190 + 440/-410	33,160	2970	287.9
241	810	29,130 + 230/-220	33,240	4110	483.9
251	1648	29,050 + 420/-400	33,520	4470	550.4
253	760	30,140 + 270/-260	33,580	3440	363.5
255	9856	29,910 + 260/-250	33,660	3750	416.7
258	9857	30,060 + 270/-260	33,780	3720	410.9
260	811	30,110 + 260/-250	33,860	3750	415.7
262	9858	30,490 + 290/-280	33,960	3470	366.8
265	9859	30,090 + 310/-290	34,080	3990	457.6
268	9860	31,030 + 340/-330	34,240	3210	321.9
270	812	31,040 + 260/-250	34,320	3280	333.1

Table 1 Marine calibration points derived from core PS2644<sup>a</sup> (Continued)

Composite depth <sup>b</sup> (cm)	Lab code (KIA-)	<sup>14</sup> C age ± 1 σ (yr BP)	GISP2 calendar age (yr BP)	Age difference (yr)	Marine Δ <sup>14</sup> C <sup>c</sup> (‰)
273	9861	31,170 + 340/-330	34,420	3250	327.7
275	761	31,580 + 500/-470	34,540	2960	280.1
283	813	31,800 + 270/-260	34,740	2940	276.0
292	814	31,950 + 280/-270	35,140	3190	314.5
297.5	75	32,080 + 1670/-1380	35,280	3200	315.5
304	815	31,930 + 280/-270	35,540	3610	383.1
312	816	32,550 + 290/-280	35,780	3230	318.1
320	817	32,410 + 330/-310	36,220	3810	414.6
325	818	33,140 + 330/-320	36,360	3220	313.7
331	819	36,160 + 360/-340	36,800	3640	382.1
340	820	33,430 + 320/-310	37,380	3950	433.6
344	821	33,920 + 350/-330	37,640	3720	391.8
354	11,257	32,580 + 240/-230	38,020	5440	721.9
357	11,256	32,650 + 270/-260	38,220	5570	748.7
359	1449	32,660 + 560/-520	38,260	5600	755.0
363	11,258	33,920 + 270/-260	38,580	4660	559.4
367	889	34,850 + 930/-840	38,800	3950	426.4
370	11,259	34,890 + 300/-290	39,020	4130	457.6
374	11,260	35,300 + 310/-300	39,320	4020	436.3
379	890	35,150 + 990/-880	39,920	4770	573.5
381	11,261	35,200 + 310/-300	40,120	4920	602.0
384	11,262	34,780 + 300/-290	40,200	5420	704.4
386	11,263	35,170 + 300/-290	40,260	5090	635.5
389 av	1552/11,264 <sup>e</sup>	32,910 ± 220	40,440	7530	1214.6
390	910	33,250 + 770/-710	40,460	7210	1127.9
392	5375	34,400 + 190/-180	40,520	6120	857.5
394	5376	34,240 + 220/-210	40,560	6320	904.1
401	5377	35,330 ± 200	40,680	5350	686.8
403	5378	35,550 ± 200	40,780	5230	661.2
405	3347	36,810 + 1160/-1020	40,840	4030	430.4
414	911	37,450 + 1400/-1190	41,080	3630	359.8
414 (b)	1644	37,740 + 1190/-1040	41,080	3340	311.5
422	891	38,990 + 1640/-1360	41,540	2550	186.8
435	912	39,210 + 1670/-1380	41,740	2530	183.0
452	11,265	40,660 + 580/-540	42,220	1560	46.7
460	913	39,710 + 1820/-1480	42,560	2850	227.5
474 av	914/5379	42,350 + 390/-370	43,280	750	-57.3
482	1553	44,140 + 2540/-1930	43,880	-260	-170.4
488 av	1554/3975	42,700 + 840/-760	44,260	1560	39.2
492 av	892/3976	43,100 + 880/-800	44,420	1720	59.5
503 av	1555/4120	44,550 + 1080/-950	44,860	710	-67.1
507 av	1556/4121	44,340 + 990/-880	45,060	1120	-19.0
530 av	915/ 4151	45,190 + 1200/-1040	45,677 <sup>f</sup>	890	-48.8

Table 1 Marine calibration points derived from core PS2644<sup>a</sup> (*Continued*)

Composite depth <sup>b</sup> (cm)	Lab code (KIA-)	<sup>14</sup> C age $\pm 1 \sigma$ (yr BP)	GISP2 calendar age (yr BP)	Age difference (yr)	Marine $\Delta^{14}\text{C}^c$ (‰)
535	4122	44,850 + 1180/–1030	45,824 <sup>g</sup>	1370	9.3
542 av	3506/ 3696	46,210 + 660/–610	46,660	850	–56.7
549 av	3507/ 3697	45,920 + 650/–600	47,040	1520	23.9
580 av	3509/ 3699	48,840 + 960/–860	49,220	780	–73.3
627 av	3763	51,180 + 1700/–1400	52,380	1600	14.9
657 av <sup>f</sup>	3761/ 3979	52,470 + 1670/–1380	53,261	990	76.8
665 av <sup>f</sup>	3764/ 3980	51,560 + 1480/–1250	53,261	2100	–62.2

<sup>a</sup>Notes: <sup>14</sup>C ages are in Libby years ( $T_{1/2} = 5568$  yr) and not reservoir corrected. (b): ages measured on benthic foraminifera; av = weighted average (see Voelker et al. 1998 and Voelker 1999 for single dates); <sup>b</sup> composite depth scale resulting from core fit between giant boxcore (GKG) and gravity core (SL) is achieved by adding 6 cm to original gravity core depths (Voelker 1999). <sup>c</sup> not atmospheric level, because <sup>14</sup>C ages are not corrected for reservoir effect. <sup>d</sup> interpolated between <sup>14</sup>C ages from 133 and 137 cm (Voelker et al. 1998). <sup>e</sup> KIA11,264  $32,850 \pm 240$ . <sup>f</sup> ages for North Atlantic Ash Zone 2. <sup>g</sup> calendar ages based on linear interpolation between age control points (Voelker 1999).